# Decision-making under uncertainty in the early phase of building façade design based on multi-objective stochastic optimization

Chujun Zong[a,*,1], Manuel Margesin[a], Johannes Staudt[a], Fatma Deghim[a] and Werner Lang[a]

[a]Institute of Energy Efficient and Sustainable Design and Building, Technical University of Munich, Arcisstraße 21, Munich, 80333, Germany

ARTICLE INFO

*Keywords*:
Optimization
Stochastic programming
Life cycle assessment
Uncertainty
Decision-making

ABSTRACT

In response to the European 2030 climate and energy policy framework and to satisfy various stakeholders, trade-offs between different goals should be considered in the planning phase of a building. In the early design phase, uncertainties are inevitable and should be modeled in the decision-making process. Especially for early modeling using building information modeling tools, it is of interest to find out appropriate "placeholder" materials. In this paper, we proposed a multi-objective stochastic optimization (MOSO) framework for decision-making in the early design phase of building façade design under uncertainty. Herein, two types of uncertainty were included: uncertainty in design decisions and environmental uncertainty. Coupled with a multi-criteria decision-making (MCDM) strategy, the framework aims to narrow down the possibilities of the material choice and to provide possibly robust solutions. Categorical and continuous parameters were considered to achieve three objectives: life cycle assessment in form of global warming potential, life cycle cost and thermal transmittance. Through a case study with solid timber and brick construction types, the proposed framework was validated. Results show that the insulation and outer wall cladding are the most varying parameters of the Pareto-optimal solutions for building façade design. In general, an environmental advantage in solid timber construction and an economic advantage in solid brick construction can be seen. With the established framework, decision-making considering dynamic changes during the planning process can be potentially realized in future works.

## 1. Introduction

Globally, building sector accounts for almost half of the total primary energy consumption and for about one third of the $CO_2$ emissions [1]. In many developed countries, buildings play a more dominant role in energy consumption than both industry and transport, presumably due to a higher standard of comfort in the built environment [2]. To change the course of situation, the European Union initiated the 2030 climate and energy policy framework to raise ambitious targets of greenhouse gas emission reduction, increase in renewable energy use and improvement in energy efficiency [3]. Nevertheless, studies show that aiming at energy reduction can result in an extensive use of materials [4, 5]. This can consequently lead to an increase in embodied energy consumption and $CO_2$ emissions throughout a building's whole life cycle. Moreover, reducing investment costs is often observed as one of the most important goals for property owners when encountering design decisions in reality. Hence, in response to the 2030 climate and energy policy framework and to satisfy various stakeholders, design solutions considering relevant trade-offs are expected [6].

Mathematically, problems containing two or more conflicting goals are denoted as multi-objective optimization (MOO) problems. In this context, a set of Pareto-optimal solutions is generated for decision-makers, instead of one unique solution. In conventional methods, MOO problems are often converted into single-objective optimization (SOO) problems through strategies like the weighted sum method [7]. In contrast, multi-objective evolutionary algorithms (MOEAs) have gained increasing attention for their ability of finding multiple Pareto sets. MOEAs have entered into the limelight since Schaffer [8] proposed a vector-evaluated genetic algorithm, which enables the combination of genetic algorithms and MOO. Nowadays, industrial applications have often applied elitist MOEAs, such as non-dominated sorting genetic algorithm II (NSGA-II) [7]. Other MOEAs like particle-swarm optimization (PSO) and strength Pareto evolutionary algorithm (SPEA and SPEA-II) also play a dominant role in this area.

In the last decade, MOEAs were widely applied in the building industry to solve MOO problems, which often include objectives such as operational energy performance [9–11], thermal comfort [9, 10, 12], daylight conditions [13, 14], life cycle assessment (LCA) [11, 15–19] and life cycle cost (LCC) [10, 17–19]. This directly indicates the benefit of investigating MOO problems in the praxis of the building industry. According to statistics, the most studied objective is operational energy performance, while relatively fewer MOO studies investigated the aspects of LCA [20]. Herein, despite of the slightly simple and crude classification, two different kinds of impact indicators can be classified in the broad definition of LCA: parameters describing the use of resources and environmental impact indicators. The LCA parameters in the related MOO approaches usually referred to the latter.

Abdou et al. [10] used NSGA-II to find optimal energy efficiency net zero energy building solutions considering the global warming potential (GWP, i.e. $CO_2$ emissions) and LCC. Waibel et al. [18] also aimed at minimizing cost and GWP in the design process with a similar approach, where

*Corresponding author
chujun.zong@tum.de (C. Zong)
ORCID(s):

different design parameters including building geometry were investigated and $\epsilon$-constraint method was applied. Ciardiello et al. [17] further investigated the building geometry optimization considering objectives of GWP, cost and operational energy. In [15], Azari et al. took into account possibly many impact indicators including GWP, ozone depletion potential (ODP), acidification potential (AP), eutrophication potential (EP) and smog formation potential (SFP). Operational energy consumption was also included and assessed through dynamic building simulations using eQuest. In more recent studies, the variety of parameters and objectives has grown. In addition to LCC and operational energy, indoor thermal comfort has also become one of the key optimization objectives. Gagnon et al. [16] combined LCC, embodied and operational $CO_2$ emissions with occupants' thermal comfort as objective functions in the optimization process, in the form of long-term percentage of dissatisfied person (LPD). In [12], thermal comfort was taken into account besides energy balance, GWP and return of investment. In 2022, Fan et al. [13] investigated the optimal façade solution considering shading ratio, operational energy and daylight comfort using SPEA-II. Similarly, De Luca et al. [14] conducted a multi-objective optimization study of non-operable shading systems focusing on the visual comfort.

As stated in most studies, an MOO problem is particularly relevant in early design phases because Pareto-optimal solutions can be offered in advance. However, certain uncertainties are inevitable in the early stages of planning and should be modeled, which most of the afore-mentioned studies failed to consider. Some other studies analytically studied the uncertainty of building geometry in the early design phase [17, 21, 22]. Nevertheless, tentative material choice of building components is also necessary, especially for the early modeling process. Compared to other modeling tools, building information modeling (BIM) tools are gaining increasing attention when conducting an LCA calculation during the development process of a building [23]. Studies show that planers often work with placeholder materials when modeling in early design stages, especially when dealing with several projects at the same time. Consequently, random choices of the placeholder materials will lead to a less meaningful design assistance of an LCA calculation based on Bill of Quantities from the building model [24]. Thus, it is of interest to find possibly robust optimal solutions of material choice for planners working on a vast number of projects through an MOO under uncertainty.

In general, uncertainty can be included in the optimization process in two ways: *a posteriori* and *a priori*. Sensitivity analysis, as one of the classical *a posteriori* approaches, was commonly applied in the analysis of the built environment [11, 12, 25, 26]. In MOO problems in particular, a post-optimization sensitivity analysis is usually applied to assess the robustness of the model or of the obtained solutions. In [25], Mukkavaar and Shadram conducted a sensitivity analysis to assess the design decisions considering trade-offs between operational and embodied energy consumption. However, primarily as an evaluation tool, the application of the sensitivity analysis method in the optimization process is greatly limited. Hence, certain studies also experimented *a priori* approaches. Chang et al. [12] used parametric modeling and Bayesian multilevel modeling to integrate uncertainty parameters into the objective functions. In [27], despite the lack of the optimization process, a new promising best-worst method was applied to deal with the uncertainty occurring in the multi-criteria decision-making process. In [26], material and environmental uncertainties were modelled in the MOO process to obtain the most cost-efficient and environmental-friendly retrofit solutions. Herein, robust optimization (RO) was applied, approximated with a surrogate-assisted Kriging model to reduce the computational cost and accelerate the optimization process.

As one of the approaches to solve optimization problems under uncertainty in operations research of applied mathematics, RO is risk-averse, which focuses on optimizing the "worst-case" scenario [28]. In contrast, stochastic optimization, i.e. stochastic programming (SP), is an alternative risk-neutral approach, which can formulate the true problem as an approximated optimization problem of an expected value (EV) function [29]. As such, the SP method enables an integration of uncertainty parameters into the optimization modeling process and seeks for optimal solutions less conservatively.

In this paper, based on MOO and SP, we propose a multi-objective stochastic optimization (MOSO) framework for decision-making under uncertainty in the early phase of building façade design. The framework is also coupled with a multi-criteria decision-making (MCDM) strategy based on the technique for order preference by similarity to ideal solution (TOPSIS). The framework helps to narrow down the possibilities of the material choice for building owners and could assist planners by providing possibly robust solutions in the early design phase. The focus of the current study is on the following aspects:

- addressing material decisions of façade design and modeling process through an MOEA, including categorical and continuous design parameters
- including LCA, LCC and thermal transmittance characteristics of potential materials as objectives
- integration of uncertainties in the early design phase using an SP approach
- proposal of optimal decisions for design assistance through a TOPSIS-based MCDM

## 2. Methodology

As presented in Fig. 1, the proposed framework consists of four main parts. First, the design parameters and uncertainty parameters were defined. The obtained parameters were then implemented into the MOSO model to give rise to

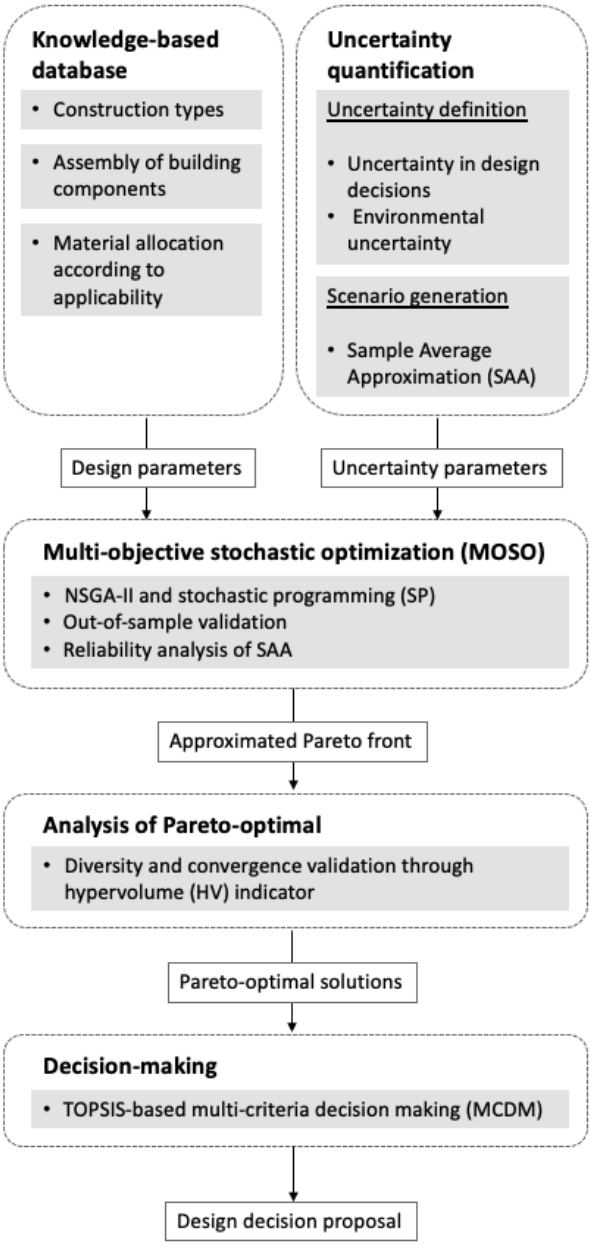


**Figure 1:** Methodological framework of MOSO to obtain optimal material decisions in the early design phase

the Pareto-optimal solutions. Through the following analysis and decision-making strategy, the choices of optimal material combination were obtained.

## 2.1. Knowledge-based database

As the data basis for the proposed framework, an expert-knowledge-assisted database was developed and case-specific design parameters can be derived from this database (exemplarily illustrated in Fig. 2) [30]. In the bottom layer of the database structure, potential building materials with the corresponding LCA information and thermal conductivity ($\lambda$-value) of each material were included. The LCA information was extracted from the publicly accessible German database Ökobaudat 2020 II. According to EN-15978 [31], the whole life cycle of a building includes stages of production (A1-A3), construction (A4-A5), end-of-life (C1-C4) and additional information outside of the life cycle (D). Within the scope of this paper, focusing on the embodied impacts, the LCA was investigated in form of GWP of the life cycle phases of production (A1-A3), disposal (C3 and C4) and production of replacement products during the reference study period. Herein, A1-A3, C3 and C4 were based on the data availability of Ökubaudat. The production of replacement products during the reference study serves as a simplified representation of the usage stage B4, which was expressed as the frequency of replacement, of which the calculation is based on the reference study period ($t$) and the reference service life (RSL) of respective material.

Next, possible applicability / functionality types (e.g. finish, wall cladding, etc.) were inputted with expert knowledge and matched to each material. Accordingly, both material and applicability related information was implemented in the data structure. The database also included thickness, unit cost of each material in applicability types for the LCA and LCC calculation, where the cost depends on the thickness of each material. It is worth mentioning that the thickness represents the thickness of the materials which are in or converted into 1 $m^2$. As a knowledge-based input, the thickness was given in ranges, whereas RSL and cost were based on data from [32, 33] and [34, 35] respectively.

The applicability types were then combined to form various sub-components for each building component (e.g. exterior wall, ceiling). Herein, each building component could be assembled in different sub-component combinations, depending on the knowledge-based inputs of assembly possibilities and main construction materials. In total, four main construction materials with detailed classification of construction types were included: timber, brick, steel and reinforced concrete. The classification of the building components in the database followed the principle of the cost groups in the German standard DIN 276 and enables a composition of an entire building by all defined building components [36].

Within the scope of this paper, the investigation focus is to find the optimal design solution of certain sub-component considering possible material combinations of its corresponding applicability types.

## 2.2. Multi-objective optimization

As aforementioned, problems with more than two conflicting goals are denoted as MOO problems. In building industry, important goals include: reduction of negative environmental impact (LCA), satisfaction of building owners regarding investment cost (LCC) and reduction of operational energy consumption. In this paper, LCA was mainly investigated within the scope of GWP. The energy performance is indicated by the thermal transmittance (U-value), which is one of the most important components of the simplified one-dimensional heat conduction equation, and the importance of estimating it during the design phase is evident [37, 38]. As stated, the design parameters are

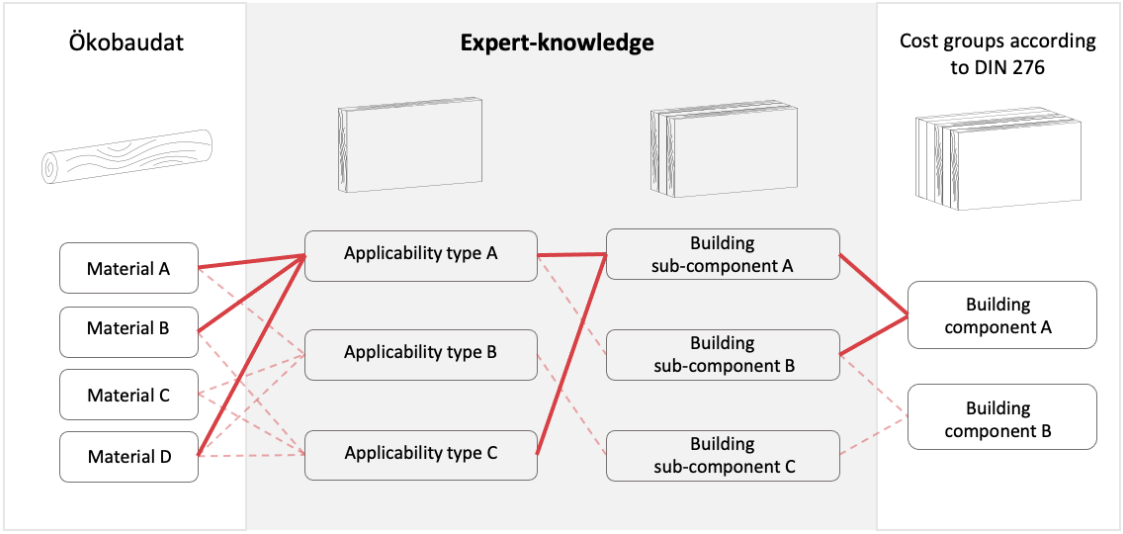


**Figure 2:** Structure of the expert-knowledge-assisted database

derived from the knowledge-based database including the material choice and its corresponding thickness of respective applicability types of the investigated sub-component. While the former is a categorical design parameter, the latter is a continuous one. Accordingly, the MOO problem is formed as (1):

$$\begin{aligned} &\min_{x\in X, d\in D} \sum_{i=1}^{N} g(x_i)\cdot d_i \cdot \frac{t}{l(x_i)} \\ &\min_{x\in X, d\in D} \sum_{i=1}^{N} c(x_i, d_i)\cdot \frac{t}{l(x_i)} \\ &\min_{x\in X, d\in D} \frac{1}{R_{se}+\sum_{i=1}^{N}\frac{d_i}{lmd(x_i)}+R_{si}} \\ &s.t. \quad \frac{1}{R_{se}+\sum_{i=1}^{N}\frac{d_i}{lmd(x_i)}+R_{si}} \le U \end{aligned} \tag{1}$$

where, in order of precedence, the objective functions are minimizing GWP, LCC and thermal transmittance of the building component. The categorical design parameter $x_i$ stands for the material of the $i^{th}$ applicability type, whereas the continuous design parameter $d$ represents the respective thickness. The GWP ($g$), cost ($c$), thermal conductivity ($lmd$) and the RSL of materials ($l$) of respective applicability are fixed values for each material and are expressed as a function of the material. Based on the reference study period ($t$) and RSL ($l$) the frequency of replacement was calculated.

In addition, the presented MOO problem is constrained by a pre-defined U-value, calculated through the heat transfer coefficient (R-value) which is expressed as $\frac{d_i}{lmd(x_i)}$. The constraint depends on regulations of different energy standards. In the proposed framework, two German energy standards were considered: nearly zero-energy building (NZEB) and German Building Energy Act (GEG).

The applied MOEA is NSGA-II, realized through the Python-based package *pymoo* [39]. As one of the most popular elitist MOEAs, NSGA-II outperforms other algorithms for its computation speed [7]. If the dominance relationship of $a$ over $b$, i.e. $a \succ b$ is valid, it is to satisfy the following condition:

$$\left\{\forall k := f_k(a) \ge f_k(b)\right\} \wedge \left\{\exists h := f_h(a) > f_h(b)\right\} \tag{2}$$

this means that $a$ is strictly better than $b$ in at least one objective, while not inferior to $b$ in all objectives [15, 40]. Specifically in NSGA-II, the crowded-comparison operator serves to maintain the diversity among solutions from the same non-dominated front and prioritizes solutions with a better non-domination rank or in less crowded areas [7].

For all genetic algorithms (GA), the determination of parameter ratios is crucial for successful research outcomes [41, 42]. The parameters include population size and search parameters such as crossover and mutation operators. Studies showed that certain optimal parameter ratios are suitable for different population sizes [41]. According to the initial settings of the NSGA-II in [7], we used simulated binary crossover (SBX) operator and polynomial mutation (PLM) operator in this study. Based on the research in [41], the corresponding probabilities were set as 0.8 and 0.01 respectively, where the crowding degree was 20. In addition, the population size was 100. The termination criterion is to be defined case-specifically based on the change in the performance indicator hypervolume (HV) during the iteration. The HV measures the area dominated by a set of solutions and bounded by a pre-defined reference point, and indicates the performance of the results regarding both diversity and convergence [43]. In this paper, the reference point was defined as (1,1,1).

When dealing with real-world problems, the Pareto front is to be approximated through multiple simulations, which

were defined as five simulation runs in this paper. The obtained solution sets were analyzed and evaluated through the HV value, and the Pareto set with the highest HV value was further analyzed in the MCDM procedure.

## 2.3. Uncertainty quantification

Uncertainties arise from the lack of information or knowledge about the true value of certain variables and occur during the early planning phase of a building [44,45]. In this paper, inspired by previous studies [26,46,47], two main kinds of uncertainties were defined: uncertainty in design decisions and environmental uncertainty. As aforementioned, the investigation focus within the scope of this paper is to find the optimal design solution of certain sub-component. As components (e.g. exterior wall) are sometimes viewed in their entirety, for example, in order to calculate U-values, uncertainty in design decisions can arise when the choice of the material combination for other sub-components within the component, in which the sub-component under study is located, has not yet been determined at the time of decision-making. These uncertainties can be due to the uncontrollable nature of design preferences and due to the lack of information on project-related force majeure, such as static calculation, fire protection regulations, etc. These uncertainties are expressed as the cumulative GWP ($\xi_{gwp}$), costs ($\xi_c$) and R-values ($\xi_r$) of other sub-components that are not to be optimized. On the other hand, environmental uncertainties refer to changes in the parameters that are objectively determined only by environmental factors, such as weather and time [46]. Herein, no direct influence of design decisions is present. In this study, environmental uncertainty $\xi_{rsl}$ is represented as the uncertain RSL of the applicability type that is in direct contact with the outside. The information on this is based on the data from [48]. The two types of uncertainties were integrated in the aforedescribed MOO problem using an SP approach.

## 2.4. Stochastic programming

In general, an SP problem is presented as follows [29, 49]:

$$\min_{x\in X, X\in\mathbb{R}^m, \xi\in\mathbb{R}^n} \left\{ F(x) := \mathbb{E}_P[f(x,\xi)] \right\} \tag{3}$$

where $F(x)$ is the EV function of the problem corresponding to the true valued function $f(x,\xi)$ [29]. In our case, the MOSO problem is formed as:

$$\begin{aligned} &\min \left[\mathbb{E}_P[f_1(x,d,\xi)],\ \mathbb{E}_P[f_2(x,d,\xi)],\ \mathbb{E}_P[f_3(x,d,\xi)]\right] \\ &s.t. \quad \mathbb{E}_P[g(x,d,\xi)] \le U \end{aligned} \tag{4}$$

where $f_1$, $f_2$ and $f_3$ represent GWP, cost and thermal transmittance respectively, and $g$ stands for the constraint. $x$ and $d$ represent the design parameters, in our case the material and the corresponding thickness. The random vector $\xi$ stands for the uncertainty parameters. In principle, the probability distribution $P$ of each random vector $\xi$ is assumed to be known *a priori*. In problems where $P$ can be interpreted discretely, the EV function can be formed as [29]:

$$\mathbb{E}_P[f(x,\xi)] = \sum_{j=1}^{N} p_j f(x,\xi_j). \tag{5}$$

Herein, different scenarios $\xi_j$ with respective probabilities $p_j$, $j = 1, ..., N$ from the probability distribution $P$ are to be generated.

## 2.5. Scenario generation

Despite possible finite support of the probability distribution of uncertainty parameters, solving SP problems can still be computationally intensive. One of the popular techniques to generate scenarios is using the exterior Monte Carlo (MC) sampling approach to approximate the true value [29]. The idea is to draw $N$ pseudo-random samples $\xi_k$ from the *a priori* obtained probability distribution $P$ such that the general problem (3) is approximated by:

$$\begin{aligned} &\min_{x\in X, X\in\mathbb{R}^m, \xi\in\mathbb{R}^n} \left\{ \hat{F}_N(x) := \frac{1}{N}\sum_{k=1}^{N} f(x,\xi_k) \right\} \\ &s.t. \left\{ \hat{G}_N(x) := \textstyle\sum_{k=1}^{N} g(x,\xi_k) \le 0 \right\} \end{aligned} \tag{6}$$

which is denoted as a sample average approximation (SAA) approach [29, 49–52]. In such way, a SP problem can be transformed into a deterministic optimization problem and be solved. In this study, if the probability distribution function (PDF) of the uncertainty parameters can be fitted, the SAA approach will be performed; otherwise, the parameters will be integrated into the problem using (5).

By integrating uncertainty parameters through SP, the MOO problem becomes an MOSO problem.

## 2.6. Validation of stochastic programming

According to the Law of Large Numbers, $F(x)$ of problem (3) can be approximated by $\hat{F}(x)$ as $N \to \infty$ [29]. Nevertheless, since $\infty$ is impossible to reach and in order to reduce the computational and time cost, the sample size $N$ should be determined. In this paper, sample sizes of $N =$ 50, 100, 500, 1,000, 5,000 were tested respectively.

Subsequently, it is necessary to check if the sample size $N$ is large enough. For this purpose, the out-of-sample validation approach is introduced. For the validation, a set of samples (i.e. validation set) is used, where the sample size $M$ is bigger than the sample size $N$ under study. In SOO problems, it is to evaluate the proximity of $\hat{F}(x)$ and obtained $F_{val}(x)$ through the validation set. If $\hat{F}(x) \approx F_{val}(x)$ does not hold, $N$ should be increased. In our case, within an MOSO problem, the comparison of $\hat{F}(x)$ and $F_{val}(x)$ was realized through a three-dimensional and pair-wise two-dimensional illustrations of the approximated Pareto fronts. Accordingly, a validation set with 10,000 samples was defined. The sample size can then be selected that provides satisfactory performance without being extremely time-consuming.

In addition to the out-of-sample validation, the optimization outcomes were validated regarding the reliability of the SAA approach, where the impact of the potentially interdependent uncertainty parameters on the optimization results was examined. Herein, MC simulation was performed 1,000 times with the exact discrete optional design parameters and the average values of each objective function were compared with the corresponding optimization results.

### 2.7. Multi-criteria decision-making

In the early design phase, it is intended to provide planners with possible optimal solutions for free subjective selection. However, sorting out the priority of the obtained Pareto-optimal solutions can also better help the decision-makers. For this purpose, techniques such as MCDM are usually applied [25, 40, 53]. Through numeric techniques, MCDM methods help to rank a discrete set of potential options and assist decision-makers to make optimal decisions.

In this paper, an Euclidean-distance-based method, TOPSIS, was applied. Before performing the TOPSIS method, it is necessary to establish weighting factors for each target and normalize the results. In the first step, the results of the obtained Pareto-optimal options were normalized through:

$$s_{ki} = \frac{f_{ki} - \min(f_{ki})}{\max(f_{ki}) - \min(f_{ki})} \tag{7}$$

which is denoted as the Max-Min method, for which the maximum and minimum values of the results were required. Here, $f_{ki}$ represents the result of the $k^{th}$ objective in the $i^{th}$ order. As for determining the weighting factor, two kinds of methods were used in this study. The first one is the entropy weight method (EWM), where the entropy for each objective is calculated as [54]:

$$E_k = -\frac{1}{\ln n} \sum_{i=1}^{n} s_{ki} \ln s_{ki} \tag{8}$$

where $n$ represents the number of results under each objective, in our case the population size (100) of the MOSO. Subsequently, the weighting factor $w$ for each objective is defined as [54]:

$$w_k = \frac{1 - E_k}{\sum_{k=1}^{m}(1 - E_k)} \tag{9}$$

Beside the EWM, as a comparison, the weighting factor of each objective was also manually defined to represent the decision-makers' preference for certain one or two objectives.

In the procedure of the TOPSIS method, the "ideal" ($s_k^+$) and the "nadir" ($s_k^-$) points, i.e. the best and the worst results of each objective, should primarily be defined. Then, the Euclidean distance of each result to the "ideal" and the "nadir" points was calculated respectively following the equations [55]:

$$d_i^+ = \sqrt{\sum_{k=1}^{m}(s_{ki} - s_k^+)^2} \tag{10}$$

$$d_i^- = \sqrt{\sum_{k=1}^{m}(s_{ki} - s_k^-)^2} \tag{11}$$

Subsequently, the relative closeness to the ideal solution, i.e. the so-called score, is presented as follows [55]:

$$c_i = \frac{d_i^-}{d_i^- + d_i^+},\ 0 < c_i < 1 \tag{12}$$

Among the obtained Pareto-optimal solutions, the alternative solution with a $c_i$ closest to 1 will be selected as the best solution. Other alternative solutions will be listed in order of the score. Accordingly, a set of ranked optimal solutions can be provided to planners / decision-makers.

## 3. Case Study

### 3.1. Construction type

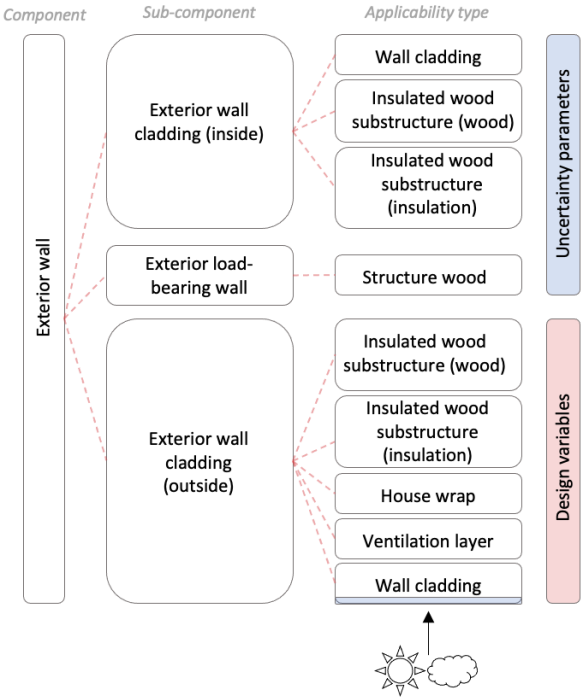


**Figure 3:** Investigated solid timber construction type

For the case study, the exterior wall of solid timber and brick construction types with ventilated façade elements was investigated, which are one of the most commonly applied conventional construction types [56]. As stated, the frequency of replacement was calculated based on the reference

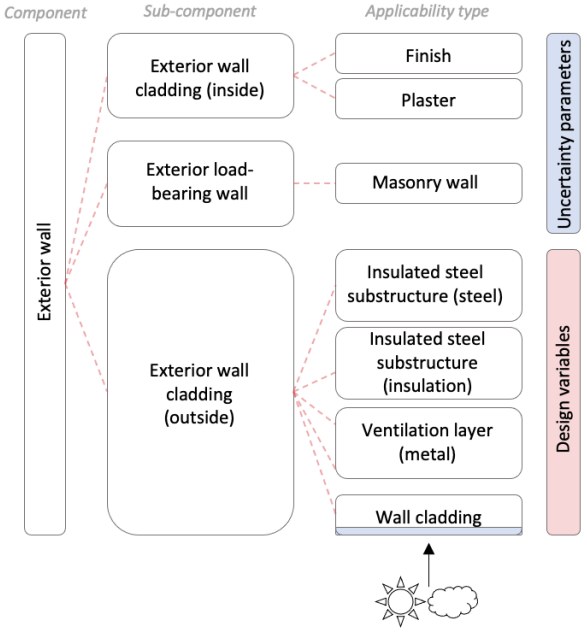


**Figure 4:** Investigated solid brick construction type

study period and RSL from the knowledge-based database. In the case study, the reference study period was defined as 55 years. It is to mention that since the investigated façade elements were ventilated, the applicability types on the outer side of the ventilation layer were not included in the calculation of the thermal transmittance. The required data were extracted from the corresponding part of the knowledge-based database. As shown in Figure 3 and Figure 4, the building component exterior wall consists of three sub-components: exterior wall cladding (inside), exterior load-bearing wall, and exterior wall cladding (outside). From the top to the bottom, the elements are arranged in order from the inside to the outside of a building. Depending on different inputted construction types, various applicability types were allocated to each sub-component. Herein, it is to note that additional interior insulation is commonly needed for the installation layer in timber construction, while brick walls are often of simpler construction with only exterior insulation. Thus, double the exterior insulation thickness was defined for the brick construction to obtain two rigorously qualitatively equivalent construction types. Regardless of the main construction materials, the sub-component exterior wall cladding (outside) is observed as the aesthetic, insulating and sheltering layer against weathering changes. Hence, it is of interest to find the possibly most robust option of this sub-component, especially when other sub-components are uncertain in the early stages or subject to changes as the design process progresses. Accordingly, the respective material choice for each applicability type of the exterior wall cladding (outside) were the design parameters $x_i$, while the cumulative GWP ($\xi_{gwp}$), costs ($\xi_c$) and R-values ($\xi_r$) of the other sub-components of the exterior wall were considered as uncertainties in design decisions.

### 3.2. Parameter quantification

The following is a detailed description of solid timber construction as an example. In total, 10 design parameters were defined for the solid timber construction (Table 1). The materials of the applicability types of the sub-component exterior wall cladding (outside) are categorical parameters, while the respective corresponding thickness is counted as a continuous parameter. As mentioned in section 2.1, all materials are in or converted into 1 $m^2$ and the thickness were therefore subsequently adjusted. Accordingly, the wooden or metal part of the substructure are converted from slats and profiles to plates. In addition, the thickness range of house wrap is exactly 1, for the GWP unit of the materials assigned to this applicability type were "kg $CO_2$-eq/$m^2$", and the thickness considered in the subsequent calculation maintained consistent. In this case, the cost was not thickness-dependent.

As shown in Figure 3 and 4, the parameters marked with blue are the uncertainty parameters, including the applicability types from exterior wall cladding (inside), exterior load-bearing wall and the RSL of the wall cladding on the outer side. For uncertainty in design decisions, potential materials of all uncertain applicability types were merged by order and subsequently by their matching sub-components. The merging in this context was based on the Cartesian product of all the uncertain material decisions. To prevent the dimensional explosion of the Cartesian product, we defined the maximum, minimum and average values for the thickness of each uncertain material. Accordingly, the probability distribution $P$ can be obtained for each uncertainty parameter. Subsequently, the cumulative GWP values ($\xi_{gwp}$), costs ($\xi_c$) and R-values ($\xi_r$) of the sub-components exterior wall (inside) and the exterior load-bearing wall were defined. As for the environmental uncertainty parameters, the wall cladding on the outer side is most affected by the environment and weather among all applicability types. Hence, its RSL was observed as the environmental uncertainty parameter $\xi_{rsl}$ in this study. The drawn pseudo-random samples followed the log normal distribution based on [48].

### 3.3. Energy standard

As aforementioned, two energy standards were taken into account in the study. Depending on certain regional regulations or requirements from the building owners, different U-values of building components are accepted. For the exterior wall, the required U-value from GEG and NZEB is 0.21 W/$m^2$K and 0.18 W/$m^2$K respectively. With these two different constraints, the respectively obtained Pareto-optimal solutions from the MOSO process were compared.

## 4. Results

### 4.1. Uncertainty quantification

Through the Cartesian product of all the uncertain material choices, possible combinations of the exterior wall cladding (inside) and exterior load-bearing wall, i.e. the uncertainty parameters in design decisions, were obtained.

**Table 1**
Design parameters of solid timber construction ((15),(16) and (17) are products from the manufacturer ROCKWOOL)

| Design parameters | Description | Parameter type | Parameter set |
|---|---|---|---|
| $x1$ | House wrap | categorical | (1) PE underlay - fabric reinforced (thickness 0.00015m)<br>(2) PP underlay (thickness 0.00015m)<br>(3) PUR underlay on PET fleece (thickness 0.0005m) |
| $x2$ | Ventilation layer (wood) | categorical | (5) Softwood lumber - dried<br>(6) Beech lumber (12% moisture, 10.7% $H_2O$)<br>(7) Spruce lumber (12% moisture, 10.7% $H_2O$)<br>(8) Pine lumber (12% moisture, 10.7% $H_2O$)<br>(9) Larch lumber (12% moisture, 10.7% $H_2O$) |
| $x3$ | Insulated wood (insulation) | categorical | (10) Conventional cotton<br>(11) Ecological cotton<br>(12) Flax fleece<br>(13) Hemp fleece<br>(14) Mineral wool (façade insulation)<br>(15) rock wool insulation in high density range<br>(16) rock wool insulation in medium density range<br>(17) rock wool insulation in low density range |
| $x4$ | Insulated wood (wood) | categorical | (18) Softwood lumber - dried<br>(19) Beech lumber (12% moisture, 10.7% $H_2O$)<br>(20) Spruce lumber (12% moisture, 10.7% $H_2O$)<br>(21) Pine lumber (12% moisture, 10.7% $H_2O$)<br>(22) Larch lumber (12% moisture, 10.7% $H_2O$) |
| $x5$ | Wall cladding | categorical | (23) Aluminum sheet<br>(24) Steel hot rolled sheets (2-20mm)<br>(25) Steel sheet (20 µm strip galvanized)<br>(26) Steel sheet (0.3-3mm)<br>(27) NedZink Naturel<br>(28) NedZink NOVA, NedZink NOIR<br>(29) Stainless steel sheet<br>(30) Lead sheet<br>(31) Oak lumber (12% moisture, 10.7% $H_2O$)<br>(32) Planed timber<br>(33) Hardwood lumber<br>(34) Softwood lumber<br>(35) Natural stone slab, hard, façade, (thickness 0.03m)<br>(36) Natural stone slab, soft, façade<br>(37) WPC façade element<br>(38) Beech lumber (12% moisture, 10.7% $H_2O$)<br>(39) Spruce lumber (12% moisture, 10.7% $H_2O$)<br>(40) Pine lumber (12% moisture, 10.7% $H_2O$)<br>(41) Larch lumber (12% moisture, 10.7% $H_2O$)<br>(42) TERRART façade panel<br>(43) Cast glass - profile construction glass<br>(44) Cast glass - basic profile construction glass<br>(45) Hot dip galvanized steel sheet<br>(46) Fiber cement board<br>(47) Pladur |
| $x6$ | Thickness of house wrap | continuous | [1,1] |
| $x7$ | Thickness of Ventilation layer (wood), unit: m | continuous | [0.0016, 0.0064] |
| $x8$ | Thickness of insulated wood (insulation), unit: m | continuous | [0.0276, 0.092] |
| $x9$ | Thickness of insulated wood (wood), unit: m | continuous | [0.0024, 0.008] |
| $x10$ | Thickness of wall cladding, unit: m | continuous | Material-specific |

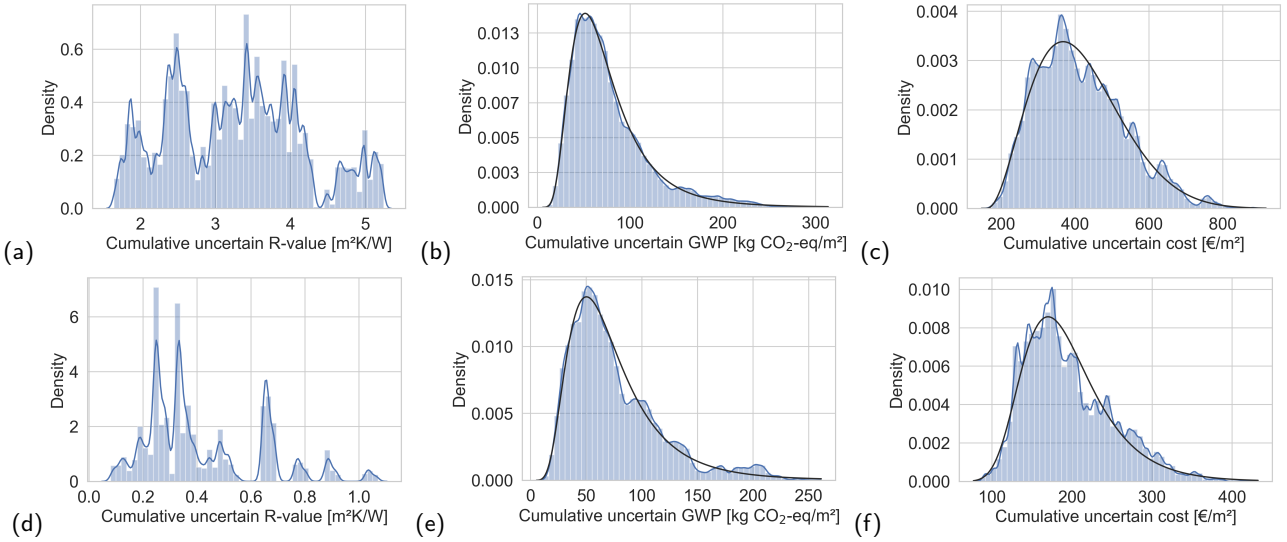


**Figure 5:** Probability distribution of uncertainty parameters of solid timber construction: (a) cumulative R-value, (b) cumulative GWP, (c) cumulative cost of sub-components exterior wall cladding (inside) and exterior load-bearing wall; and of solid brick construction: (d) cumulative R-value, (e) cumulative GWP, (f) cumulative cost of sub-components exterior wall cladding (inside) and exterior load-bearing wall

**Table 2**
Fitting results of uncertainty parameters of solid timber construction

| Uncertainty parameter | Description | Fitted PDF | Fitting parameters |
|---|---|---|---|
| $\xi_r$ | R-value | - | - |
| $\xi_{gwp}$ | GWP | F distribution | loc: -0.21, dfn: 26.74, dfd: 12.33, scale: 64.96 |
| $\xi_c$ | Cost | $\chi^2$ distribution | df: 11.61, loc: 124.22, scale: 25.03 |
| $\xi_{rsl}$ | RSL Wall cladding | Log normal distribution | meanlog: 3.78, sdlog: 0.34 [48] |

**Table 3**
Fitting results of uncertainty parameters of solid brick construction

| Uncertainty parameter | Description | Fitted PDF | Fitting parameters |
|---|---|---|---|
| $\xi_r$ | R-value | - | - |
| $\xi_{gwp}$ | GWP | F distribution | loc: -0.17, dfn: 20.06, dfd: 13.09, scale: 64.46 |
| $\xi_c$ | Cost | Gumbel distribution | loc: 169.93, scale: 42.91 |
| $\xi_{rsl}$ | RSL Wall cladding | Log normal distribution | meanlog: 3.78, sdlog: 0.34 [48] |

The results were then analyzed through a probability distribution fitting with the Python-based package *fitter*, and the best fitted PDF was selected based on the squared sum of error (SSE). Fig. 5 shows the probability distribution of the uncertainty parameters, i.e. cumulative R-value, cumulative GWP, and cumulative cost of sub-components exterior wall cladding (inside) and exterior load-bearing wall. While the cumulative R-value of the solid timber construction does not fit any common PDF, the latter two uncertainty parameters were proven to fit the F distribution and $\chi^2$ distribution respectively. As for the solid brick construction, similarly, the R-value does not fit any common PDF, while the cumulative GWP and cumulative cost fit the F distribution and Gumbel distribution respectively. When comparing the two construction types, it is interesting to observe that the probability distribution course of the uncertainty parameters is similar for timber and brick construction. A possible explanation lies in the similar solid construction type and the ventilated façade elements.

The fitting results are shown in Table 2 and Table 3. Accordingly, the quantification of the cumulative uncertain R-values can be realized through the (5) in section 2.3.1, while the other uncertainties can be determined through the SAA approach.

## 4.2. Termination criterion

In this paper, the termination criterion of the MOSO is determined according to the HV value during the iteration.

Figure 6 shows the change in the HV value of timber construction during one exemplary run. Starting from an initial population size of 15,000, obtained through the Cartesian product of the categorical parameters, the population size increased in steps of 100. Here, a significant rise of the HV value was observed during the first 18,000 function evaluations, i.e. 30 generations, and a gradual stabilization from approximately the $19{,}000^{th}$ function evaluation, i.e. the $40^{th}$ generation. Based on this and to ensure a better stability, the termination criterion was defined as 100 iterations. Similarly, the termination criterion for brick construction was set at 100 generations based on the gradual stable point of HV value.

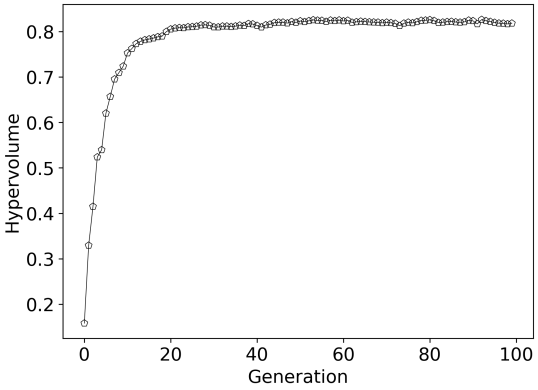


**Figure 6:** Hypervolume during generation increase of solid timber construction constrained by the energy standard NZEB

### 4.3. Pareto-optimal solutions

Through the proposed method, the approximated fronts of the two construction types, each constrained by the two energy standards, can be obtained. Figure 7 exemplarily shows the results of solid timber construction constrained by NZEB. Herein, the out-of-sample validation is illustrated through the three-dimensional comparison of $\hat{F}(x)$ of sample sizes $N = 50$, 100, 500, 1,000, 5,000, with the $F_{val}(x)$ of 10,000 samples. It can be observed that the approximated Pareto fronts resembled the validation set at a sample size of 1000, which suggests a further procedure with this sample size. To better interpret the out-of-sample validation result, an exemplary two-dimensional projection is shown in Fig. 8.

From the results obtained, the "best" performing Pareto set was selected in each case according to the HV value. The selected solution sets of timber construction, constrained by NZEB and GEG, had HV values of 0.82 and 0.78, respectively. As for brick construction with NZEB and GEG constraints, the solution sets with HV value of 0.78 and 0.76 were selected. The obtained Pareto-optimal solutions are shown in the supplementary material, which can be provided to planners or decision-makers as design assistance support during the early design and modeling phase.

For timber construction, the material options for house wrap and the wooden plate of the ventilation layer are relatively limited in all scenarios. In contrast, more material solutions were provided for the insulated wood substructure and wall cladding. For the insulation part of the insulated wood substructure, the most commonly appearing material is rock wool insulation in low density range. Especially to satisfy the constraint of NZEB, almost half of the 100 Pareto-optimal solutions contain this insulation material. The reasons for this result point to the significantly lower price and GWP of this material. For the wooden part of the insulated wood substructure, softwood lumber is most often selected to meet the requirements of NZEB (73%) and GEG (92%). Since the potential materials are merely slightly different regarding cost and thermal conductivity, softwood lumber outperforms other materials for its low GWP value in total. As for wall cladding, there are 7 and 6 materials covering wood, metal and glass for the contraints of NZEB and GEG respectively. It can be observed that the frequency of occurrence of steel and wooden materials is similar.

For brick construction, the choice of material is relatively definite for the steel part of the insulated steel substructure and the metal part of the ventilation layer. Similar to timber construction, more material options were obtained for insulation and wall cladding. The insulation materials that appeared most frequently to satisfy the NZEB constraint are rock wool insulation in low and in high density range, and for the GEG constraint it is rock wool insulation in low density range. As for the wall cladding, similar results to those obtained for timber construction were obtained, with a slight predominance of hardwood timber.

Concerning the continuous parameters, the obtained thickness of each material varies within a relatively smaller range than its initially defined range. This is especially pronounced in insulation materials, due to the constrained thermal transmittance of the exterior wall. Evidently, because of a more lenient constraint, the range of results to achieve GEG is larger than that for achieving NZEB to a certain extent. For instance, in timber construction, rock wool insulation in low density range has a range between 7.7 cm and 9.2 cm for NZEB, and a range between 5 cm and 9.2 cm for GEG. Regardless of the different ranges for the different energy standards, the narrowed thickness ranges lie above their average thickness values defined in the knowledge-based database. This is consistent with the argument about the value of SP in a side perspective, that decisions made using only the average of the parameters are not optimal [57]. In our case, a more supported choice of material thickness can be offered for building modeling in the early planning phase.

In addition, it is to observe that conventional cotton, the insulation material with the lowest maximum cost, the second lowest GWP yet the highest thermal conductivity, was additionally accepted for both construction types under GEG constraint. This is due to the less stringent constraint of GEG, which leads to a greater tolerance to materials with relatively higher thermal conductivity and a preference for materials with better performance on the other two objectives. When comparing the objective outcomes, i.e. EVs of the exterior wall, the results vary by the main structure material in

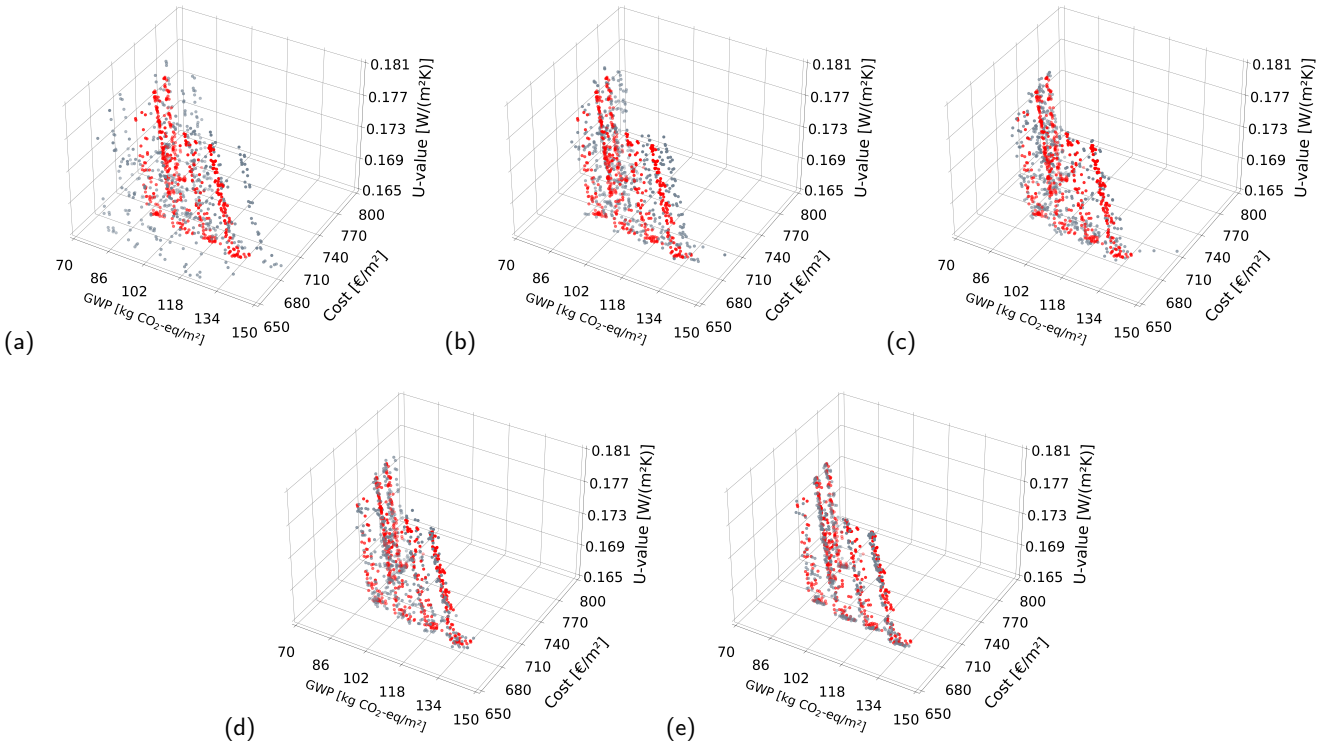


**Figure 7:** Out-of-sample validation results of solid timber construction constrained by NZEB (the red point cloud represents the validation set with 10,000 samples, the gray point clouds represent investigated sample sizes): (a) sample size 50, (b) sample size 100, (c) sample size 500, (d) sample size 1000, (e) sample size 5000

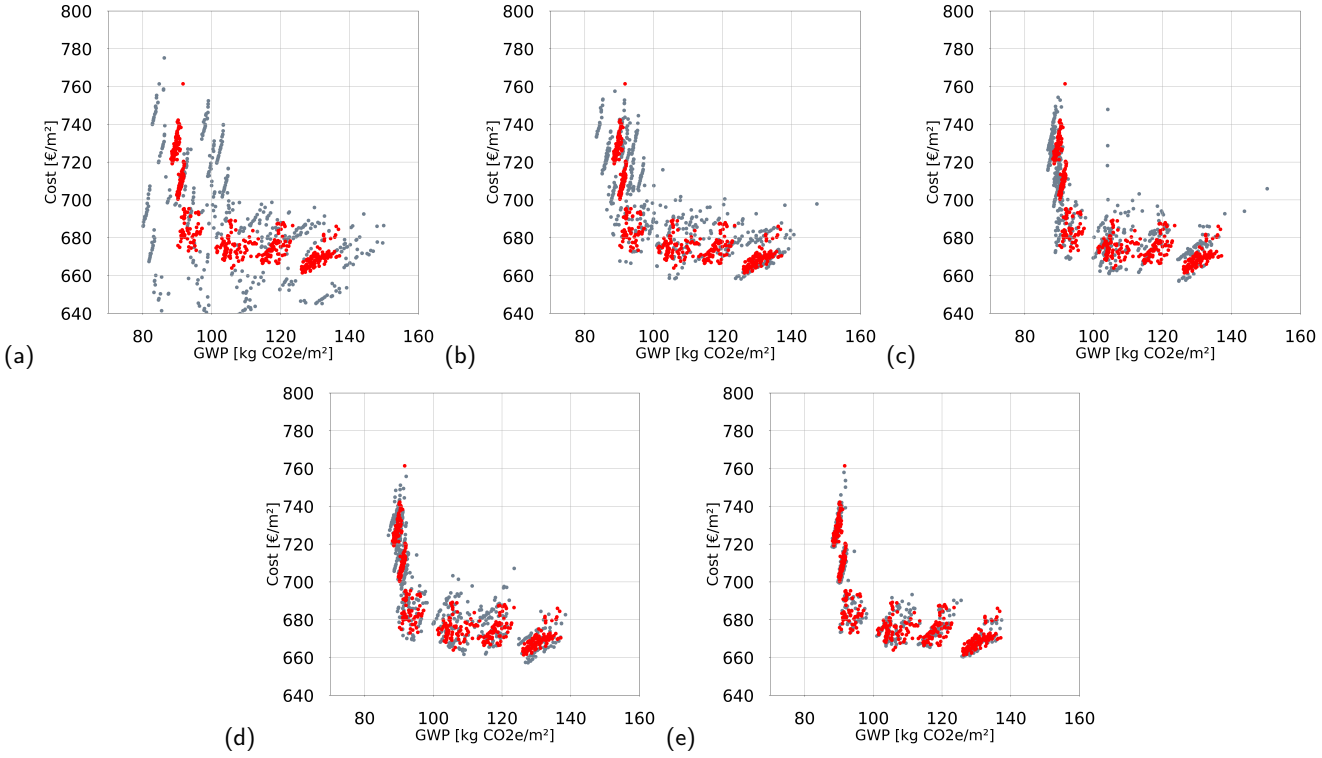


**Figure 8:** Exemplary two-dimensional projection of the out-of-sample validation results of solid timber construction constrained by NZEB: (a) sample size 50, (b) sample size 100, (c) sample size 500, (d) sample size 1000, (e) sample size 5000

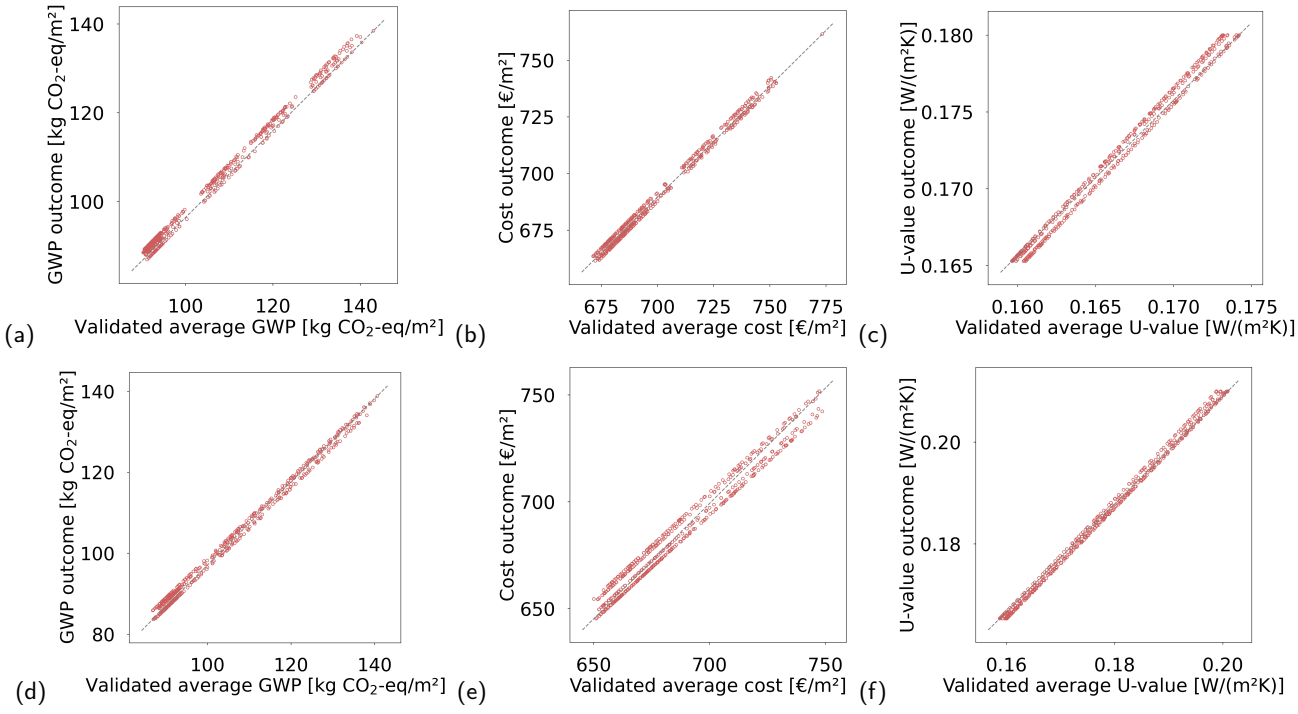


**Figure 9:** Reliability analysis of the optimization results of timber construction through the SAA approach: (a)-(c) constrained by NZEB, (d)-(f) constrained by GEG

spite of the similar solid construction and ventilated façade elements. Subject to the constraints of thermal transmittance being satisfied, timber construction has generally lower expected GWP values, while brick construction demonstrates its overall price advantage.

### 4.4. Validation of stochastic programming

Beside the afore-shown out-of-sample validation, the results of the reliability analysis of the SAA approach were performed. Figure 9 exemplarily shows the results of the solid timber construction. It is to observe that the average GWP, cost and U-value results from the MC simulation are consistent with the optimized outcomes, which proved the reliability of the SAA approach. In addition, this analysis is especially valuable since the uncertainty parameters were based on specific characteristics of the materials and could be potentially interdependent. In this respect, the applied methodology was proved feasible and reliable in case of having potentially interdependent uncertainty parameters.

### 4.5. Decision-making

Following the method described in section 2.4, the obtained 100 Pareto-optimal options were further analyzed and sorted in descending order. For this purpose, 14 scenarios with different weighting factors and energy standards were compared for each construction type. The respective weighting factors are shown in Table 4. Regarding the results using the EWM, it is to mention that the choice of the normalization method could affect the outcome of the weighting factors. Since we applied the Max-Min method, the weighting factors vary in a relatively even range. In addition to the weighting factors based on EWM, weighting factors to mimic the decision-makers' preference were defined. In this respect, the factor for the higher weighted criterion is 0.8 if one objective is preferred and 0.45 respectively if two objectives are preferred.

**Table 4**
Weighting factors of the objectives

| Method | GWP | Cost | U-value |
|---|---|---|---|
| EWM (timber, NZEB) | 0.34 | 0.36 | 0.3 |
| EWM (timber, GEG) | 0.31 | 0.39 | 0.3 |
| EWM (brick, NZEB) | 0.3 | 0.42 | 0.29 |
| EWM (brick, GEG) | 0.324 | 0.317 | 0.359 |
| GWP dominated | 0.8 | 0.1 | 0.1 |
| Cost dominated | 0.1 | 0.8 | 0.1 |
| U-value dominated | 0.1 | 0.1 | 0.8 |
| GWP-cost dominated | 0.45 | 0.45 | 0.1 |
| GWP-U-value dominated | 0.45 | 0.1 | 0.45 |
| Cost-U-value dominated | 0.1 | 0.45 | 0.45 |

Table 5 and Table 6 show the optimal options for the two construction types in different scenarios. It is worth noting that since all objectives have weighting factors in all cases, the results of scenarios with preferred objective(s) are not equal to results from an SOO process. Generally for timber construction, it is to observe that the optimal solutions under all scenarios constrained by NZEB are similar, with mineral wool and rock wool insulation in low density range alternating for the insulation. In contrast, the material combinations for GEG are more diverse. Due to a more

**Table 5**
The optimal option for timber construction under each scenario (all materials are in or converted into 1 $m^2$)

| Scenario | Insulated wood substructure (wood) | Insulated wood substructure (insulation) | House wrap | Ventilation layer (wood) | Wall cladding | GWP (kg $CO_2$-eq/$m^2$) | Cost (€/$m^2$) | U-value (W/$m^2$K) |
|---|---|---|---|---|---|---|---|---|
| EWM (NZEB) | Softwood lumber 0.008 m | rock wool insulation in low density range 0.092 m | PP underlay | Softwood lumber 0.006 m | Hardwood lumber 0.015 m | 92.71 | 689 | 0.165 |
| GWP dominated (NZEB) | Softwood lumber 0.008 m | rock wool insulation in low density range 0.092 m | PP underlay | Softwood lumber 0.006 m | Hardwood lumber 0.015 m | 92.71 | 689 | 0.165 |
| Cost dominated (NZEB) | Softwood lumber 0.008 m | Mineral wool (façade insulation) 0.092 m | PP underlay | Softwood lumber 0.002 m | Hardwood lumber 0.015 m | 96.51 | 680 | 0.166 |
| U-value dominated (NZEB) | Softwood lumber 0.008 m | Mineral wool (façade insulation) 0.092 m | PP underlay | Softwood lumber 0.002 m | Hardwood lumber 0.015 m | 96.51 | 680 | 0.166 |
| GWP-cost dominated (NZEB) | Beech lumber 0.008 m | rock wool insulation in low density range 0.089 m | PE underlay | Softwood lumber 0.002 m | Hardwood lumber 0.015 m | 93.39 | 677 | 0.169 |
| GWP-U-value dominated (NZEB) | Softwood lumber 0.008 m | rock wool insulation in low density range 0.092 m | PP underlay | Softwood lumber 0.006 m | Hardwood lumber 0.015 m | 92.71 | 689 | 0.165 |
| Cost-U-value dominated (NZEB) | Softwood lumber 0.008 m | Mineral wool (façade insulation) 0.092 m | PP underlay | Softwood lumber 0.002 m | Hardwood lumber 0.015 m | 96.51 | 680 | 0.166 |
| EWM (GEG) | Softwood lumber 0.008 m | rock wool insulation in low density range 0.092 m | PE underlay | Softwood lumber 0.006 m | Softwood lumber 0.015 m | 91.24 | 748 | 0.165 |
| GWP dominated (GEG) | Softwood lumber 0.008 m | Conventional cotton 0.091 m | PE underlay | Softwood lumber 0.002 m | Hardwood lumber 0.016 m | 94.08 | 681 | 0.177 |
| Cost dominated (GEG) | Softwood lumber 0.008 m | Conventional cotton 0.088 m | PE underlay | Softwood lumber 0.002 m | Steel sheet (0.3-3mm) 0.0005 m | 106.79 | 671 | 0.179 |
| U-value dominated (GEG) | Softwood lumber 0.008 m | Mineral wool (façade insulation) 0.09 m | PE underlay | Softwood lumber 0.002 m | Hardwood lumber 0.015 m | 96.48 | 691 | 0.168 |
| GWP-cost dominated (GEG) | Softwood lumber 0.005 m | rock wool insulation in low density range 0.052 m | PP underlay | Softwood lumber 0.002 m | Steel sheet (0.3-3mm) 0.0005 m | 101.67 | 657 | 0.208 |
| GWP-U-value dominated (GEG) | Softwood lumber 0.008 m | Mineral wool (façade insulation) 0.09 m | PE underlay | Softwood lumber 0.002 m | Hardwood lumber 0.015 m | 96.48 | 691 | 0.168 |
| Cost-U-value dominated (GEG) | Spruce lumber 0.008 m | rock wool insulation in high density range 0.092 m | PP underlay | Softwood lumber 0.002 m | Steel sheet (0.3-3mm) 0.0005 m | 134.31 | 679 | 0.166 |

lenient constraint, insulation with smaller thickness (e.g. 5.2 cm) or with higher thermal conductivity (e.g. conventional cotton) was occasionally selected for the optimal solutions. In addition, the difference in material combination for scenarios with one preferred objective and scenarios with two preferred objectives can be seen. For instance, when looking at the results of scenarios constrained by NZEB, if cost was the only preferred objective, the insulation material with the lowest price (conventional cotton) was chosen without regard to other objectives; if U-value is equally weighted, the least expensive insulation material with relatively low thermal conductivity (rock wool insulation in high density range) was chosen instead. As for brick construction, the results present a similar picture as for timber construction. To satisfy the constraint of NZEB, rock wool insulation in low density range was top-ranked. To meet the requirement of GEG, conventional cotton appears often for its price

**Table 6**
The optimal option for brick construction under each scenario (all materials are in or converted into 1 $m^2$)

| Scenario | Insulated steel substructure (steel) | Insulated steel substructure (insulation) | Non-insulated metal substructure (metal) | Wall cladding | GWP (kg $CO_2$-eq/$m^2$) | Cost (€/$m^2$) | U-value (W/$m^2$K) |
|---|---|---|---|---|---|---|---|
| EWM (NZEB) | Hot dip galvanized steel sheet | rock wool insulation in low density range 0.198 m | Aluminium profile 0.0004 m | Hardwood lumber 0.015 m | 137.4 | 567 | 0.16 |
| GWP dominated (NZEB) | Hot dip galvanized steel sheet | rock wool insulation in low density range 0.195 m | Aluminium profile 0.0003 m | Hardwood lumber 0.015 m | 131.99 | 566 | 0.162 |
| Cost dominated (NZEB) | Hot dip galvanized steel sheet | rock wool insulation in low density range 0.19 m | Aluminium profile 0.0003 m | Steel sheet (0.3-3mm) 0.0005 m | 146.64 | 556 | 0.166 |
| U-value dominated (NZEB) | Hot dip galvanized steel sheet | rock wool insulation in low density range 0.198 m | Aluminium profile 0.0004 m | Hardwood lumber 0.015 m | 137.4 | 567 | 0.16 |
| GWP-cost dominated (NZEB) | Hot dip galvanized steel sheet | rock wool insulation in low density range 0.196 m | Aluminium profile 0.0003 m | Hardwood lumber 0.015 m | 131.99 | 566 | 0.162 |
| GWP-U-value dominated (NZEB) | Hot dip galvanized steel sheet | rock wool insulation in low density range 0.198 m | Aluminium profile 0.0004 m | Hardwood lumber 0.015 m | 137.4 | 567 | 0.16 |
| Cost-U-value dominated (NZEB) | Hot dip galvanized steel sheet | rock wool insulation in low density range 0.198 m | Aluminium profile 0.0004 m | Hardwood lumber 0.015 m | 137.4 | 567 | 0.16 |
| EWM (GEG) | Hot dip galvanized steel sheet | Conventional cotton 0.17 m | Aluminium profile 0.0003 m | Hardwood lumber 0.015 m | 129.06 | 531 | 0.207 |
| GWP dominated (GEG) | Hot dip galvanized steel sheet | rock wool insulation in low density range 0.193 m | Aluminium profile 0.0002 m | Hardwood lumber 0.015 m | 128.5 | 568 | 0.164 |
| Cost dominated (NZEB) | Hot dip galvanized steel sheet | Cotton conventional 0.198 m | Aluminium profile 0.0002 m | Steel sheet (0.3-3mm) 0.0005 m | 146.91 | 534 | 0.181 |
| U-value dominated (NZEB) | Hot dip galvanized steel sheet | rock wool insulation in low density range 0.193 m | Aluminium profile 0.0002 m | Hardwood lumber 0.015 m | 128.5 | 568 | 0.164 |
| GWP-cost dominated (NZEB) | Hot dip galvanized steel sheet | Conventional cotton 0.192 m | Aluminium profile 0.0003 m | Hardwood lumber 0.015 m | 131.86 | 538 | 0.186 |
| GWP-U-value dominated (NZEB) | Hot dip galvanized steel sheet | rock wool insulation in low density range 0.193 m | Aluminium profile 0.0002 m | Hardwood lumber 0.015 m | 128.5 | 568 | 0.164 |
| Cost-U-value dominated (NZEB) | Hot dip galvanized steel sheet | rock wool insulation in high density range 0.198 m | Aluminium profile 0.0003 m | Steel sheet (0.3-3mm) 0.0005 m | 204.85 | 547 | 0.161 |

advantage, as long as the constraint of thermal transmittance is satisfied.

Overall, although the other top-ranked material combinations for each construction type and energy standard differ from scenario to scenario, some degree of overlap can be observed in the top-ranked material combinations. Despite certain similarity, the top-ranked Pareto-optimal options vary the most in insulation and wall cladding choice, regardless of scenarios and energy standards. While the thickness of the same wall cladding materials remains the same for the same energy standard, the thickness of the insulation materials vary. This can be explained by its thickness and its importance in terms of thermal transmittance, which also confirms the rationale for optimizing the chosen

building sub-component. The most frequently top-ranked insulation material is rock wool insulation in low density range, whereas conventional cotton is top-ranked in cost dominated scenarios. Furthermore, hardwood lumber generally outperforms other wall cladding materials. When observing the objective outcomes of the top-ranked options, it is to see that the respective GWP and price advantages of timber and brick construction types resonate the results in section 4.3.

Based on the frequency of occurrence of the optimal option in scenarios with different weighting factors, the best solution for timber construction, in the order of applicability types in Fig. 5, is the combination of softwood lumber, rock wool insulation in low density range, PP underlay, softwood lumber and hardwood lumber. As for brick construction, the best solution is the combination of softwood lumber, mineral wool, PE underlay, softwood lumber and hardwood lumber. Nevertheless, it should be noted that the top-ranked optimal solution merely provides one recommended decision option, and the entire Pareto-optimal solution set should be observed as a decision catalog for design and modeling assistance in the early design phase.

## 5. Discussion

As the decision-making considering trade-offs to satisfy various stakeholders has been gaining increasing attention in building planning process, numerous previous studies have been conducted to obtain the best design solutions through the MOO approach. However, merely limited studies have modeled the uncertainty that is inevitable in the early design phase. The presented work aims to perform a decision-making procedure in the early design phase of façade design under uncertainty. For this purpose, an MOSO framework, coupled with a TOPSIS-based MCDM strategy, was proposed to narrow the range of material choices and to target the possibly robust solutions. Focusing on the material choice, the proposed framework helps to choose the possibly robust material combination of building façade design in the early phase, which is especially useful for the early modeling process, e.g. when choosing the appropriate placeholder materials in the BIM software. Subsequently, more meaningful LCA calculation and building performance simulation could be realized. As the data basis of this study, a knowledge-based database was created to integrate expert knowledge of building construction types, composition of building components and material applicability. Compared to other studies [15,26,46], the database enables a systematic integration of the most common construction types which circumvents cumbersome case-specific analysis and is thus beneficial in other arbitrary cases in the early design phase. On the basis of the knowledge-based database, categorical and continuous design parameters could be defined to calculate the objectives of LCA, LCC and thermal transmittance.

In this paper, two types of uncertainty were defined: uncertainty in design decisions and environmental uncertainty. Compared to other studies [15, 25], the classification provides a more understandable communication and allows a better application in real decision-making process in early design stages. In addition, this contributes to provide a basis for integrating other uncertainty parameters into a more comprehensive uncertainty catalog in future studies. The uncertainty was modelled in the proposed MOO problem through an SP approach. Compared to previous studies, such as [11, 21, 25], the proposed MOSO framework provides a novel way to integrate uncertainty *a priori* in the optimization process, which effectively provides recommended options for building façade materials when considering uncertainties in decision-making. Moreover, different from the RO approach proposed by [26], the SO approach is risk-neutral and can provide optimal solutions less conservatively.

With a case study of two construction types, solid timber and brick construction, our MOSO framework was tested. Results show that regardless of construction types and energy standards, the most varying applicability types were insulation and exterior wall cladding, which were also the sharing applicability types of the two construction types. Regarding thickness, it was also proved that it is not optimal to use only the average value of the parameters in decision-making. Comparing the two construction types, when the constraints of the energy standards were satisfied, timber construction shows its advantage in GWP and brick construction is more advantageous in terms of cost. As the database is based on the German market, we encourage researchers to validate the results in an alternative economic context. In addition, the MCDM strategy allowed ranking of the obtained Pareto-optimal solutions, which can be ordered according to specific preferences of the three investigated objectives. Overall, a Pareto-optimal solution set with recommendations can be provided as a decision catalog that can potentially serve as a design guidance for planners, especially for finding appropriate "placeholder" materials in the early modeling phase.

However, certain perspectives of the presented framework can still be deepened. Since the study mainly focused on the material choice of the building façade design, other aspects were not taken into account, such as heating and cooling conditions and window-to-wall ratio, which are also relevant in the early design and modeling phase. In a follow-up study, it is intended to extend the design parameters and uncertainty parameters based on the introduced uncertainty classification. Secondly, the environmental uncertainty in this study, i.e. the RSL of the wall cladding, was defined equally for all materials. This lack of material differentiation can be filled by a more detailed investigation of the façade in segmented types, such as material types.

In a longer view, subsequent compensation measures (e.g. more insulation material or technological solutions) according to the decisions made during the design development can also be included in the proposed single-stage MOSO framework. In future work, we plan to further incorporate multi-stage decision-making and possible dynamic changes of uncertainty parameters into the framework considering a holistic design process.

## 6. Conclusion

In this paper, we proposed an MOSO framework, coupled with a TOPSIS-based MCDM strategy, to find out the possibly robust optimal material combination of building façade design in the early design and building modeling phase. Two types of uncertainty, uncertainty in design decisions and environmental uncertainty, were defined and modelled *a priori* through an SP approach. Through a case study of two construction types, it can be observed that the most varying applicability types of exterior walls were insulation and wall cladding. In addition, the proposed MOSO framework was able to demonstrate that it is not optimal to use only the average thickness of building components in optimization to support decision-making. Overall, a GWP advantage in solid timber construction and a cost advantage in solid brick construction can be observed. To conclude, the presented work establishes a foundational framework that could potentially be applied in a more dynamic decision-making process to explore in depth the decision-making under uncertainty in building design.

## 7. Acknowlegement

This research was funded by the Deutsche Forschungsgemeinschaft (German Research Foundation, DFG) under grant FOR2363—project number: 271444440. In addition, the authors would like to thank Dr. Yilun Sun for his advice and encouragement.

## References

[1] A. Costa, M. M. Keane, J. I. Torrens, and E. Corry, "Building operation and energy performance: Monitoring, analysis and optimisation toolkit," *Applied energy*, vol. 101, pp. 310–316, 2013.

[2] L. Yang, H. Yan, and J. C. Lam, "Thermal comfort and building energy consumption implications–a review," *Applied energy*, vol. 115, pp. 164–173, 2014.

[3] E. Commission, "A renovation wave for europe—greening our buildings, creating jobs, improving lives," 2020.

[4] P. Chastas, T. Theodosiou, and D. Bikas, "Embodied energy in residential buildings-towards the nearly zero energy building: A literature review," *Building and environment*, vol. 105, pp. 267–282, 2016.

[5] J. Kneifel, E. O'Rear, D. Webb, and C. O'Fallon, "An exploration of the relationship between improvements in energy efficiency and life-cycle energy and carbon emissions using the birds low-energy residential database," *Energy and buildings*, vol. 160, pp. 19–33, 2018.

[6] M. Scherz, E. Hoxha, D. Maierhofer, H. Kreiner, and A. Passer, "Strategies to improve building environmental and economic performance: an exploratory study on 37 residential building scenarios," *The International Journal of Life Cycle Assessment*, pp. 1–15, 2022.

[7] K. Deb, A. Pratap, S. Agarwal, and T. Meyarivan, "A fast and elitist multiobjective genetic algorithm: Nsga-ii," *IEEE transactions on evolutionary computation*, vol. 6, no. 2, pp. 182–197, 2002.

[8] J. D. Schaffer, "Multiple objective optimization with vector evaluated genetic algorithms," in *Proceedings of the first international conference on genetic algorithms and their applications, 1985*. Lawrence Erlbaum Associates. Inc., Publishers, 1985.

[9] C. J. Lin, K.-J. Wang, T. B. Dagne, and B. H. Woldegiorgis, "Balancing thermal comfort and energy conservation–a multi-objective optimization model for controlling air-condition and mechanical ventilation systems," *Building and Environment*, p. 109237, 2022.

[10] N. Abdou, Y. E. Mghouchi, S. Hamdaoui, N. E. Asri, and M. Mouqallid, "Multi-objective optimization of passive energy efficiency measures for net-zero energy building in morocco," *Building and environment*, vol. 204, p. 108141, 2021.

[11] Y. Jung, Y. Heo, and H. Lee, "Multi-objective optimization of the multi-story residential building with passive design strategy in south korea," *Building and Environment*, vol. 203, p. 108061, 2021.

[12] S. Chang, D. Castro-Lacouture, and Y. Yamagata, "Decision support for retrofitting building envelopes using multi-objective optimization under uncertainties," *Journal of Building Engineering*, vol. 32, p. 101413, 2020.

[13] Z. Fan, M. Liu, and S. Tang, "A multi-objective optimization design method for gymnasium facade shading ratio integrating energy load and daylight comfort," *Building and Environment*, vol. 207, p. 108527, 2022.

[14] F. De Luca, A. Sepúlveda, and T. Varjas, "Multi-performance optimization of static shading devices for glare, daylight, view and energy consideration," *Building and Environment*, vol. 217, p. 109110, 2022.

[15] R. Azari, S. Garshasbi, P. Amini, H. Rashed-Ali, and Y. Mohammadi, "Multi-objective optimization of building envelope design for life cycle environmental performance," *Energy and Buildings*, vol. 126, pp. 524–534, 2016.

[16] R. Gagnon, L. Gosselin, and S. A. Decker, "Performance of a sequential versus holistic building design approach using multi-objective optimization," *Journal of Building Engineering*, vol. 26, p. 100883, 2019.

[17] A. Ciardiello, F. Rosso, J. Dell'Olmo, V. Ciancio, M. Ferrero, and F. Salata, "Multi-objective approach to the optimization of shape and envelope in building

energy design," *Applied energy*, vol. 280, p. 115984, 2020.

[18] C. Waibel, R. Evins, and J. Carmeliet, "Co-simulation and optimization of building geometry and multi-energy systems: Interdependencies in energy supply, energy demand and solar potentials," *Applied Energy*, vol. 242, pp. 1661–1682, 2019.

[19] P. Ylmén, K. Mjörnell, J. Berlin, and J. Arfvidsson, "Approach to manage parameter and choice uncertainty in life cycle optimisation of building design: Case study of optimal insulation thickness," *Building and Environment*, vol. 191, p. 107544, 2021.

[20] M. Manni and A. Nicolini, "Multi-objective optimization models to design a responsive built environment: A synthetic review," *Energies*, vol. 15, no. 2, p. 486, 2022.

[21] H. Harter, M. M. Singh, P. Schneider-Marin, W. Lang, and P. Geyer, "Uncertainty analysis of life cycle energy assessment in early stages of design," *Energy and Buildings*, vol. 208, p. 109635, 2020.

[22] L. E. Hinkle, J. Wang, and N. C. Brown, "Quantifying potential dynamic façade energy savings in early design using constrained optimization," *Building and Environment*, vol. 221, p. 109265, 2022.

[23] Y. Teng, J. Xu, W. Pan, and Y. Zhang, "A systematic review of the integration of building information modeling into life cycle assessment," *Building and Environment*, p. 109260, 2022.

[24] A. Hollberg, G. Genova, and G. Habert, "Evaluation of bim-based lca results for building design," *Automation in Construction*, vol. 109, p. 102972, 2020.

[25] J. Mukkavaara and F. Shadram, "An integrated optimization and sensitivity analysis approach to support the life cycle energy trade-off in building design," *Energy and Buildings*, vol. 253, p. 111529, 2021.

[26] A. Galimshina, M. Moustapha, A. Hollberg, P. Padey, S. Lasvaux, B. Sudret, and G. Habert, "What is the optimal robust environmental and cost-effective solution for building renovation? not the usual one," *Energy and Buildings*, vol. 251, p. 111329, 2021.

[27] M. Scherz and A. Vafadarnikjoo, "Multiple criteria decision analysis under uncertainty in sustainable construction: a neutrosophic modified best-worst method," in *IOP Conference Series: Earth and Environmental Science*, vol. 323, no. 1. IOP Publishing, 2019, p. 012098.

[28] C. Li and I. E. Grossmann, "A review of stochastic programming methods for optimization of process systems under uncertainty," *Frontiers in Chemical Engineering*, p. 34, 2021.

[29] A. Shapiro, "Monte carlo sampling approach to stochastic programming," in *ESAIM: proceedings*, vol. 13. EDP Sciences, 2003, pp. 65–73.

[30] P. Schneider-Marin, T. Stocker, O. Abele, M. Margesin, J. Staudt, and W. Lang, "Earlydata knowledge base for material decisions in building design," *Advanced Engineering Informatics*, 2022, manuscript submitted for publication.

[31] CEN, *Sustainability of construction works - Methodology for the assessment of performance of buildings - Part 1: Environmental Performance; German and English version prEN 15978-1:2021*. Beuth Verlag, 2021.

[32] *Nutzungsdauern von Bauteilen für Lebenszyklusanalysen nach Bewertungssystem Nachhaltiges Bauen (BNB)*, Federal Institute for Research on Building, Urban Affairs and Spatial Development (BBSR) at the Federal Office for Building and Spatial Development of Germany, 2011.

[33] *Leitfaden Nachhaltiges Bauen - Anlage 6: Bewertung der Nachhaltigkeit von Gebäuden und Liegenschaften*, Federal Office for Building and Regional Planning of Germany, 2001.

[34] f:data GmbH, "Baupreislexikon," 2022, https://www.baupreislexikon.de, Last accessed on 05-05-2022.

[35] R. Müller, *BKI Baukosten Gebäude Neubau 2020: Statistische Kostenkennwerte Gebäude (Teil 1)*, 1st ed. BKI Baukosteninformationszentrum, 2020.

[36] D. I. für Normung e.V., *DIN 276 Kosten im Bauwesen: Building costs, Coûts de bâtiment et de travaux publics (btp)*. Beuth Verlag, 2018.

[37] D. Bikas and P. Chastas, "the effect of the u value in the energy performance of residential buildings in greece," *Journal of Sustainable Architecture and Civil Engineering*, vol. 6, no. 1, pp. 58–65, 2014.

[38] G. Ficco, F. Iannetta, E. Ianniello, F. R. d. Alfano, and M. Dell'Isola, "U-value in situ measurement for energy diagnosis of existing buildings," *Energy and Buildings*, vol. 104, pp. 108–121, 2015.

[39] J. Blank and K. Deb, "pymoo: Multi-objective optimization in python," *IEEE Access*, vol. 8, pp. 89 497–89 509, 2020.

[40] Y. Shao, P. Geyer, and W. Lang, "Integrating requirement analysis and multi-objective optimization for office building energy retrofit strategies," *Energy and Buildings*, vol. 82, pp. 356–368, 2014.

[41] A. Hassanat, K. Almohammadi, E. Alkafaween, E. Abunawas, A. Hammouri, and V. Prasath, "Choosing mutation and crossover ratios for genetic algorithms—a review with a new dynamic approach," *Information*, vol. 10, no. 12, p. 390, 2019.

[42] S. M. Lim, A. B. M. Sultan, M. N. Sulaiman, A. Mustapha, and K. Y. Leong, "Crossover and mutation operators of genetic algorithms," *International journal of machine learning and computing*, vol. 7, no. 1, pp. 9–12, 2017.

[43] A. P. Guerreiro, C. M. Fonseca, and L. Paquete, "The hypervolume indicator: Problems and algorithms," *arXiv preprint arXiv:2005.00515*, 2020.

[44] J. Zheng and H. C. Frey, "Quantitative analysis of variability and uncertainty with known measurement error: methodology and case study," *Risk Analysis: An International Journal*, vol. 25, no. 3, pp. 663–675, 2005.

[45] L. Gabrielli and A. G. Ruggeri, "Developing a model for energy retrofit in large building portfolios: Energy assessment, optimization and uncertainty," *Energy and buildings*, vol. 202, p. 109356, 2019.

[46] M. Moustapha, A. Galimshina, G. Habert, and B. Sudret, "Multi-objective robust optimization using adaptive surrogate models for problems with mixed continuous-categorical parameters," *arXiv preprint arXiv:2203.01996*, 2022.

[47] A. Galimshina, M. Moustapha, A. Hollberg, P. Padey, S. Lasvaux, B. Sudret, and G. Habert, "Statistical method to identify robust building renovation choices for environmental and economic performance," *Building and Environment*, vol. 183, p. 107143, 2020.

[48] K. Goulouti, D. Favre, M. Giorgi, P. Padey, A. Galimshina, G. Habert, and S. Lasvaux, "Dataset of service life data for 100 building elements and technical systems including their descriptive statistics and fitting to lognormal distribution," *Data in Brief*, vol. 36, p. 107062, 2021.

[49] Z. Zhou, J. Zhang, P. Liu, Z. Li, M. C. Georgiadis, and E. N. Pistikopoulos, "A two-stage stochastic programming model for the optimal design of distributed energy systems," *Applied Energy*, vol. 103, pp. 135–144, 2013.

[50] A. Shapiro, *Stochastic programming by Monte Carlo simulation methods*. Humboldt-Universität zu Berlin, Mathematisch-Naturwissenschaftliche Fakultät …, 2000.

[51] M. B. Bagaram and S. F. Tóth, "Multistage sample average approximation for harvest scheduling under climate uncertainty," *Forests*, vol. 11, no. 11, p. 1230, 2020.

[52] R. Y. Rubinstein and A. Shapiro, "Optimization of static simulation models by the score function method," *Mathematics and Computers in Simulation*, vol. 32, no. 4, pp. 373–392, 1990.

[53] M. Wang, H. Yu, R. Jing, H. Liu, P. Chen, and C. Li, "Combined multi-objective optimization and robustness analysis framework for building integrated energy system under uncertainty," *Energy Conversion and Management*, vol. 208, p. 112589, 2020.

[54] Y. Zhu, D. Tian, and F. Yan, "Effectiveness of entropy weight method in decision-making," *Mathematical Problems in Engineering*, vol. 2020, 2020.

[55] M. Behzadian, S. K. Otaghsara, M. Yazdani, and J. Ignatius, "A state-of the-art survey of topsis applications," *Expert Systems with applications*, vol. 39, no. 17, pp. 13 051–13 069, 2012.

[56] Z. Duan, Q. Huang, and Q. Zhang, "Life cycle assessment of mass timber construction: A review," *Building and Environment*, p. 109320, 2022.

[57] J. R. Birge and F. Louveaux, *Introduction to stochastic programming*. Springer Science & Business Media, 2011.